JOURNAL OF MATERIALS SCIENCE 25 (1990) 4688–4693

Nickel-based air-firable thick-film conductors

F. SIROTTI, M. PRUDENZIATI, T. MANFREDINI*
*Department of Physics, and * Department of Chemistry, University of Modena, Via G. Campi, 213117 41100, Modena Italy*
B. GIARDULLO, W. ANZOLIN
Zanussi, Pordenone, Italy

The evolution of microstructure/composition of nickel-based thick films prepared from air-firable pastes has been investigated. Through the use of several analytical techniques it has been found that the pastes contain elemental boron and/or a boron-rich component which effectively competes with the oxidation of nickel grains. The evolution of the electrical properties of the film has also been studied. Even when the films are not made of sintered nickel grains, relatively high conductivities and high temperature coefficients of resistance were observed.

1. Introduction

Thick-film technology has grown and become important through the use of precious metal powders for conductive layers [1] because of their extraordinary chemical and physical properties and because they may be fired in air in open furnaces in continuous processes. On the other hand, development of thick-film materials and processes utilizing a base metal is still a great challenge [2]. Base metals are prone to oxidation in air at the temperatures required for the formation of the layers and adhesion to the substrates, so that generally the processing of pure layers requires firing cycles in reducing (e.g. hydrogen) or inert (e.g. nitrogen) atmospheres. Nevertheless, nickel-, chromium-, aluminium-, and copper-based inks are available which form conductive thick-films in air, with interesting physical and electrical properties; it has been claimed that this is possibly related to the relatively low peak-firing temperatures (650° C) and "passivating agents" for high-temperature exposure [3]. Applications of base-metal thick-films include cathodes in gas discharge display (mainly nickel), solar cell electrodes (e.g. aluminium), terminations of varistors, thermistors, capacitors, and other electrical components, heating elements (e.g. defrosters) and temperature sensors (mainly nickel) [4, 5].

Studies on the metallurgical aspects of film formation and their relation to the electrical properties have favoured copper-based conductors, because of the great interest in copper-interconnected multilayer systems, and in highly conductive strips for microwave circuits [6, 7].

The present work on nickel-based air-firable films aimed to study the evolution of the microstructure of the films, including interactions with alumina substrates, at various stages of the firing process, and to correlate this evolution with their performance (electrical properties and adhesion).

With this aim in mind, four different nickel-based inks, which were fired under various conditions, including peak temperatures and at times largely outside the values suggested by the manufacturers, were analysed; these procedures allowed the physico-chemical processes involved in film formation to be enhanced, making their identification easier.

2. Materials and methods

Four inks, supplied by three manufacturers, were included in this study; the pastes and the corresponding films will be referred to hereafter as G4, G3, E2 and T5. The inks were screen printed on 96% alumina (Hoechst, CeramTec 708) and 99.5% beryllia (Brush and Welldmann, Thermalox 995) substrates and fired at various firing temperatures, T_f, in the range 400 to 1000° C. Unless otherwise specified the firing cycle lasted 30 min and had a 10 min dwell time [8].

Several analytical techniques were used for investigating the composition and microstructure of the inks and the films. Thermogravimetric (TG) analysis was performed on dried inks (200° C, 2 h) in an alumina crucible, with a 10° C min^{-1} heating rate and a 1 l min^{-1} air flow. X-ray diffraction (XRD) patterns were obtained on dried and fired films, using Cu$K\alpha$ lines (E = 8.044 eV, nickel filter) by means of a Philips PW1700 diffractometer. The composition of dried and fired films was investigated using energy dispersive X-ray fluorescence (EDS), wavelength dispersive fluorescence (WDS), atomic absorption (AA) and secondary ion mass spectroscopy (SIMS). EDS analyses were performed using a scanning electron microscope (SEM, Philips 500) equipped with an Si(Li) X-ray detector having a beryllium window. Hence elements of low atomic number ($Z < 10$) could not be detected. EDS allowed us to determine the presence and distribution of aluminium, silicon, lead and nickel; measurements were performed with a 25 kV electron beam impinging on the sample surface or on its cross-section. WDS analyses were performed using an ARL-SEMQ microprobe equipped with a PbSd crystal. This technique was primarily devoted to

0022–2461/90 $03.00 + .12

the analysis of boron and oxygen, on the sample surfaces. A suitable S/N ratio was obtained with an impinging electron current of 150 nA and an electron energy of 15 keV.

Atomic absorption analyses were performed using a PV 9900 spectrophotometer on weighed dried pastes dissolved in HF/HNO_3. Boron was determined using the Azometina H colorimetric method; this analysis required different dissolution procedures according to the various pastes, as described in the next section.

Measurements of film thickness were made with a Talysurf (model 10). Sheet resistances of the samples were determined by taking mean values of four-point probe multiple measurements, as well as resistances of meander-type deposits. The results of these two types of measurement agree fairly well. The temperature coefficient of resistance (TCR) was measured on meander samples in the range -100 to $+80°$ C.

3. Results

An explorative investigation of the samples (dried pastes and fired films) was performed by means of EDS and SIMS analyses. The results show that quantitative analyses were required for boron, silicon, lead, zinc, aluminium, lithium and nickel. Quantitative data on boron concentration were obtained by the colorimetric method. In this case, dissolution in concentrated HF/HNO_3 mixture was found to be adequate for G4, G3 and T5 samples. On the contrary, E2 samples prepared by the same method showed no detectable boron in colorimetry, even though the presence of this element was known on the basis of the SIMS experiment. Consequently, a different procedure was successfully applied; the E2 paste was first attached by alkaline oxidant fusion ($NaCO_3$, $NaNO_3$ mixture) and the obtained glass dissolved in HNO_3 solution.

The different types of reactivity of the various samples suggest different forms of aggregation state for boron.

All the remaining elements, except lithium and silicon, could be quantitatively determined with AA analyses. The silica + lithia content was evaluated from the difference between the total weight and the solid residue after chemical dissolution. Taking into account also the organic content of the dried pastes (this was determined by weight loss in T_g experiments), the results of the whole compositional evaluation are reported in Table I.

The amount of nickel varied in the range 72 to 84 wt %, in the different inks. Pastes G3 and G4 are similar in composition, the main difference being in ratio Ni/B; paste T5, although similar to the previous ones, has a large lead content. E2 differs from the previous group in having a comparatively high silicon content, the presence of lithium and a different aggregation state of boron.

TABLE I Concentration (wt %) of the basic constituents of the pastes studied

	Organic	Ni	B	Pb	Zn	Al_2O_3	SiO_2 + Li_2O	Total
E2	2.62	72.64	1.53	1.30	–	3.25	18.57	99.91
T5	3.72	78.74	10.01	6.80	–	0.40		99.67
G4	4.86	83.28	6.56	4.00	0.06	0.40		99.16
G3	5.65	78.00	11.85	3.27	0.40	0.35		99.52

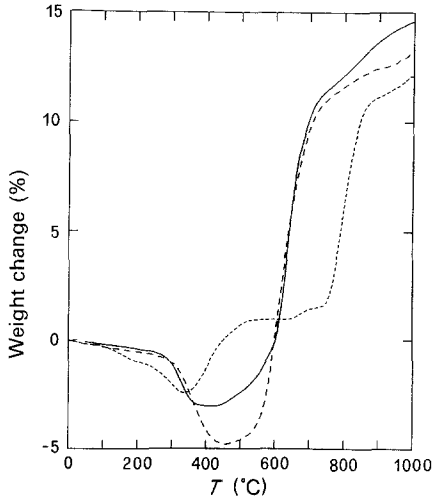

Figure 1 Thermogravimetric analysis of pastes (—) T5, (····) E2 and (– – –) G4, previously dried at 200° C.

Fig. 1 shows results of thermogravimetry of T5, E2 and G4 dried pastes. G3 inks show TG curves very similar to that shown in Fig. 1 for G4. The low temperature (200 to 400° C) weight losses are due to the organic vehicle residues (polymer) which pyrolyse in air. At higher temperatures, weight gains are observed in all the samples; however, while E2 ink exhibits three distinct steps of increase in weight, at about 430, 660 and 800° C, respectively, the other inks show a single step at about 630° C.

These weight gains suggest oxidative phenomena, whose nature was investigated using XRD and WDS analyses.

Fig. 2 shows informative parts of the XRD patterns of G4 films fired at different peak temperatures, T_f. The evolution of phases present in the layers is very complex. In dried films (spectra not shown) only reflections from nickel (JCPDS no. 4-850) are observed. At low T_f (600° C) new peaks appear due to AlB_{10} (JCPDS no. 22-2) and lead (JCPDS no. 4-686); at 750° C the reflections from lead vanish and some

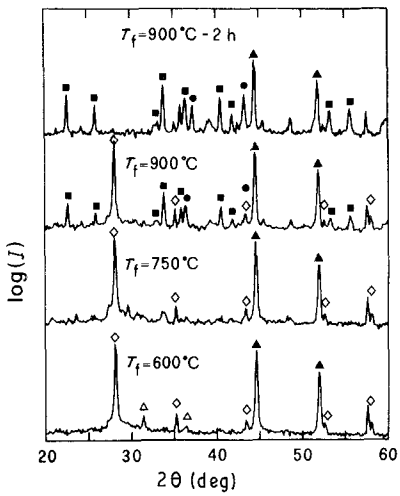

Figure 2 XRD spectra of G4 films screen printed on Al_2O_3 and fired at T_f = 600, 750 and 900° C for 10 min and at 900° C for 2 h. The reflections due to the main crystalline phases are shown: (▲) nickel, (◇) AlB_{10}, (△) Pb, (■) $Ni_3(BO_3)_2$, (●)Al_2O_3 substrate.

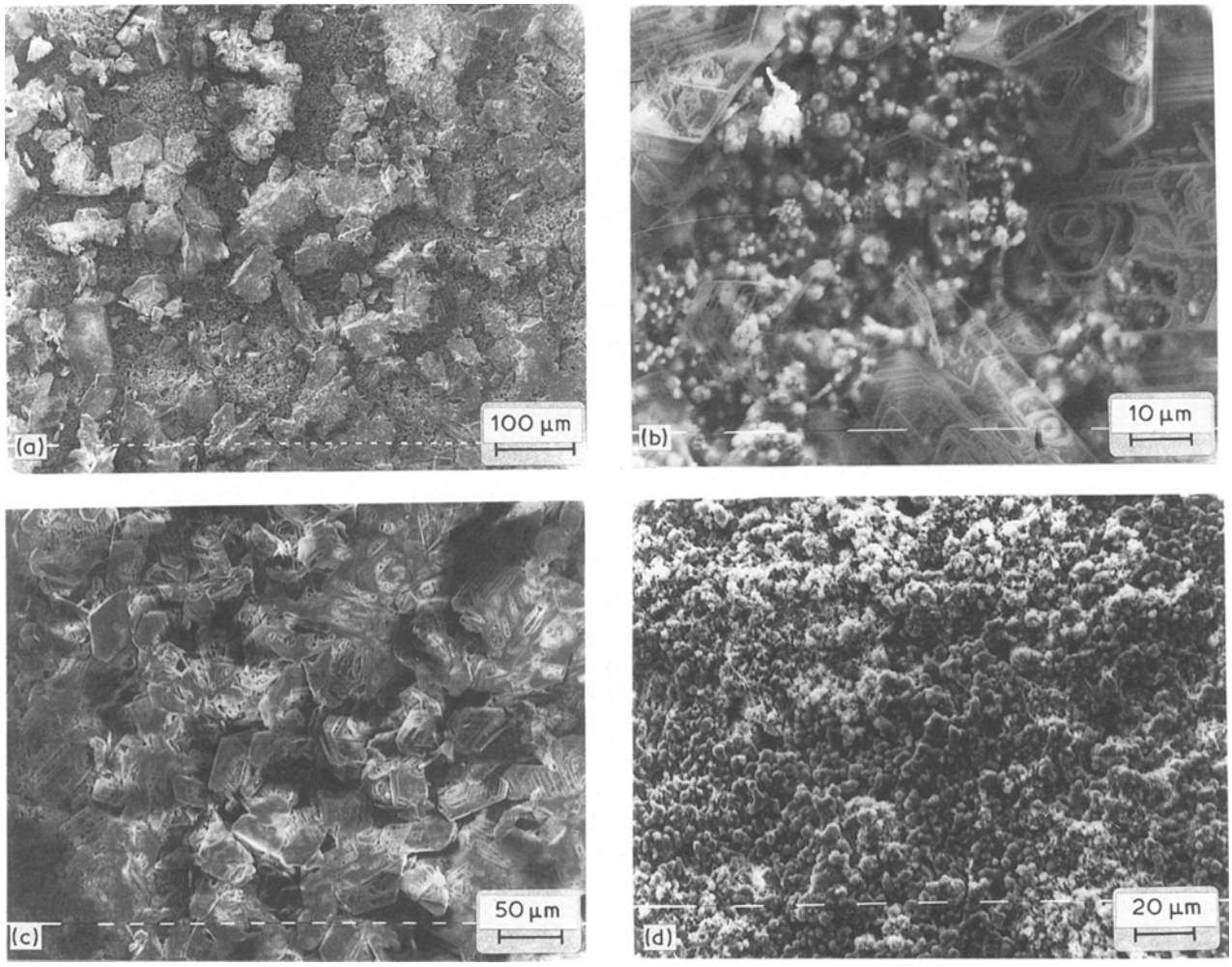

Figure 3 Surface scanning electron micrographs of the same samples in Fig. 2: (a) 600° C, 12 kV; (b) 750° C, 25 kV; (c) 900° C, 12 kV; (d) 900° C (2 h), 25 kV.

minor reflections start to be visible. Finally at higher temperatures a further phase is formed, $Ni_3(BO_3)_2$ (JCPDS no. 26-1284) and small reflections due to NiO (JCPDS no. 4-0835) are observed.

Scanning electron micrographs of surfaces of the same samples are shown in Fig. 3 where the crystalline habits of AlB_{10} crystals are observed at various temperatures. This association is supported by the finding that EDS signals are very weak when the electron beam impinges the flake-like crystals, indicating that they are made of "low Z" elements.

A very long (2 h) firing cycle at 900° C enhances the intensity of the peaks, except for those due to AlB_{10}, which vanish and thus in the SEM image (Fig. 3d) the crystalline flakes are not seen. The formation of AlB_{10} at peak temperatures in the range 750 to 900° C, as well as an increase in aluminium content detected in EDS analyses, are evidence that a film/substrate interaction occurs, with aluminium dissolution in the layer. In order to confirm this, a few films were prepared on beryllia substrates at T_f = 900° C, and analysed by XRD and EDS. The results show that in BeO-

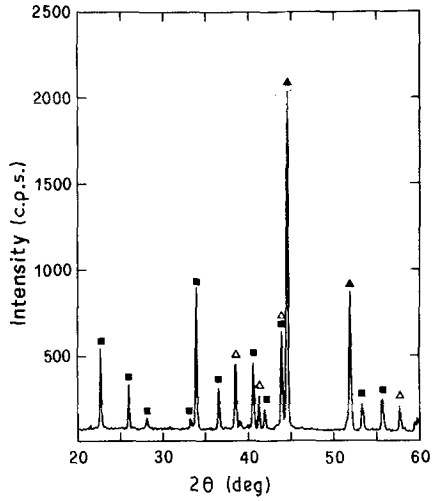

Figure 4 XRD of paste G4 screen printed on BeO substrate. (■) $Ni_3(BO_3)_2$; (▲) Ni; (△) BeO.

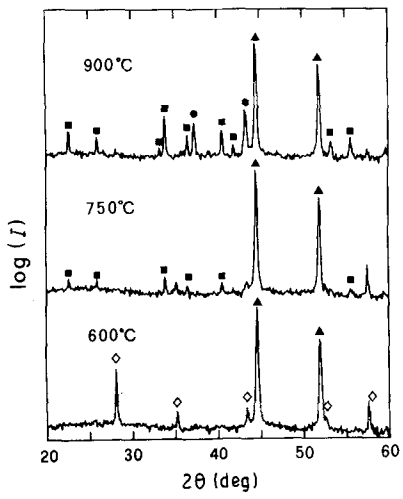

Figure 5 XRD of paste E2 screen printed on Al_2O_3 and fired at 600, 750 and 900° C for 10 min. (▲) Ni; (■) $Ni_3(BO_3)_2$; (◇) AlB_{10}.

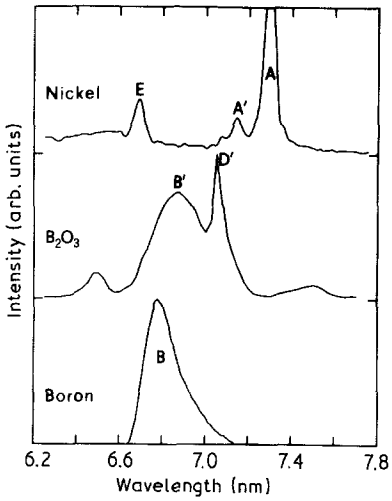

Figure 6 Reference WDS spectra of nickel, boron oxide and boron. Peak symbols correspond to: (A) Ni$L\alpha_{1,2}$, 5n; (A′) NiLβ_1, 5n; (E) NiL_1, 4n; (B) B$K\alpha$; (B′) B$K\alpha$ in B_2O_3; (D′) O$K\alpha$, 3n in B_2O_3.

supported films, only traces of aluminium are detectable and no phase involving aluminium is detected in the XRD spectra (Fig. 4).

Fig. 5 shows XRD patterns of E2 layers prepared at three different peak temperatures. In this case the same phases as observed in the previous layers are present, but their formation and dissolution temperatures are different; e.g. AlB_{10} is dissolved at lower temperatures, so that it does not give peaks at 750° C, and more NiO (larger NiO/Ni peak ratio) can be observed at 900° C.

An evaluation of the previous data left open the question concerning the nature of the oxidation phenomena, suggested by the thermogravimetric analysis. In fact, the temperature ranges for $Ni_3(BO_3)_2$ and NiO formation shown in XRD are much higher than that of weight gain in TG analysis; moreover, the amount of oxygen required to produce these oxidized phases is lower than that given by thermogravimetry.

A different explanation of the oxidation effects was found from WDS measurements. Fig. 6 shows the peaks obtained with three reference samples for elemental boron, B_2O_3 and nickel, recorded in the wavelength range 6.2 to 7.8 nm; Fig. 7 shows the spectra in the same range for the G4 and E2 films fired at two different peak temperatures (400 and 900°C),

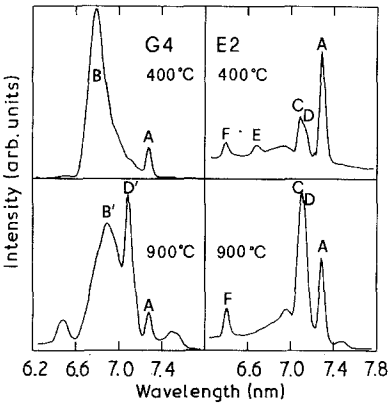

Figure 7 WDS spectra of G4 and E2 films screen printed on Al_2O_3 and fired at low (400° C) and high (900° C) temperature. (A) Ni$L\alpha_{1,2}$, 5n; (B) B$K\alpha$; (C) Si$K\alpha_{1,2}$, 10n; (D) O$K\alpha$, 3n; (E) NiL_1, 4n; (F) Si$K\alpha_{1,2}$, 9n.

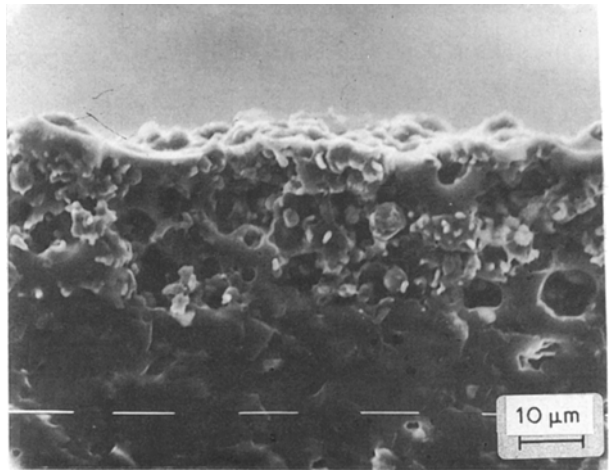

Figure 8 A scanning electron micrograph of sample E2 fired at 750° C.

the first being well below and the second above the temperature for weight gain in TG measurements. Comparison of the shape of the boron peaks (B, B′), in G4 layers with those of the references, clearly shows that at lower temperatures boron is in the elemental form, while it is in the oxidized form at higher temperatures. Similar results were found in samples prepared from G3 and T5 pastes.

WDS spectra of E2 samples prepared at 400° C include the major nickel peak (A), a peak corresponding to silicon and oxygen (C, D) and lower peaks due to nickel (E) and silicon (F). The possible contribution of boron to this spectrum merges into the background under the Si/O peak. The samples prepared at T_f = 900° C show a modified WDS spectrum, where the nickel peaks appear weaker, while the silicon peaks and especially the oxygen peak are enhanced.

Cross-sectional views of the samples in SEM show that nickel grains do not sinter in any of the films considered. As an example, Fig. 8 shows a scanning electron micrograph of sample E2 fired at 750° C. It is evident that two glassy layers are accumulated, at the conductor/substrate interface and on the top of the conductor. EDS analysis shows that these two glassy regions are rich in silicon, lead, and aluminium which is present at a concentration of nearly twice that originally present in the paste as a consequence of the interactions with the substrate.

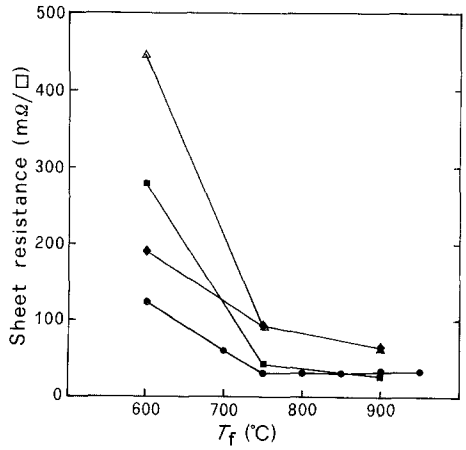

Figure 9 Sheet resistance measured in layers prepared on Al_2O_3 at various T_f. (△) G3, (■) E2, (◆) G4, (●) T5.

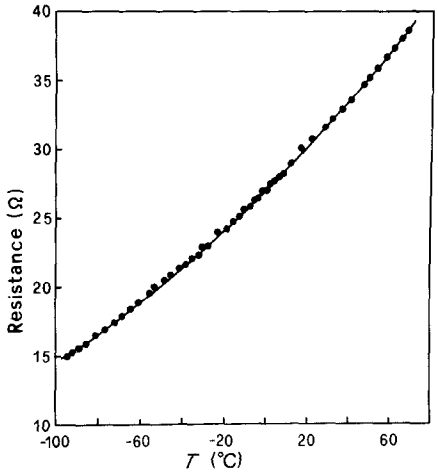

Figure 10 Resistance–temperature curve for the T5 film screen printed on Al_2O_3 and fired at 750° C.

A similar result was obtained for the other samples. In particular, lead is strongly segregated at the conductor/substrate interface in G4 layers.

3.1. Electrical characteristics

Fig. 9 shows the evolution of sheet resistance, R, of the various conductors as a function of the peak firing temperature. An increase in T_f results in a progressive decrease of resistance with a tendency to saturation for $T_f \geqslant 750°$ C. Under these conditions the resistivity values $\rho = R^* t$ (where t is the thickness of the layer) are a factor of ten higher than the resistivity of bulk nickel (about 7 $\mu\Omega$ cm [9]).

Typical behaviour of the resistance as a function of temperature is shown in Fig. 10, where it appears clearly that the data cannot be fitted by a single linear behaviour over the temperature range -80 to 80° C. However, over a shorter interval a linear response is a good approximation. We found that in the range 0 to 50° C all samples exhibit a maximum deviation from a linear interpolation lower than 1%.

The slope of these straight lines gives the TCR values, at 25° C reported in Table II where differences are seen according to the different systems. Some effect of the peak firing temperature on the TCR values of the same paste is also observed.

4. Discussion and conclusion

We have seen that air-firable nickel-based layers can be obtained starting from quite different formulations. Our compositional analysis and the results of microstructure evolution have shown that two types of system can be identified.

On the one side we have G3, G4 and T5 systems which show similar behaviour in TG, XRD and composition. In this case the film formation occurs on mixing the nickel grains with a boron powder or a boron compound which can be easily reduced during the pyrolysis of the organic vehicle. When the firing atmosphere is oxidizing after vehicle removal, elemental boron is present around the nickel grains. A competitive process of oxidation starts at T_f higher than 400° C, where boron results the more rapidly oxidized species and probably forms something like a B_2O_3 glass or a B_2O_3–PbO glass protecting the nickel powder from substantial oxidation. This is supported by WDS and XRD results. Moreover, the weight gain, ΔG_e, of a sample, computed assuming that the total amount of boron (Table I) is converted into B_2O_3, is higher than the experimental value, ΔG_m, indicating that boron oxidation is sufficient to explain the results of TG analysis. For example the computed ΔG_e for T5 is 24% and ΔG_m is 17%. In this context it is interesting that other authors [10] have found that boron powders on copper-based layers protect them from oxidation.

TABLE II TCR values measured on layers prepared at various temperatures

	T_f = 600° C	T_f = 750° C	T_f = 900° C
E2	5569	4810	5560
T5	5109	4788	5343
G4	5710	5432	5610
G3	5293	5756	5279

In E2 samples boron seems to be not the only competitor for nickel oxidation. In fact, in this case several glass-forming oxides (SiO_2, Li_2O, Al_2O_3) and elements (boron, lead) are present in the paste and a glassy matrix is formed at low temperatures. No clear scheme can be proposed for correlations between the weight gains (three steps in Fig. 1) and the oxidation of chemical species. Also, in this case, boron could be partially responsible for some oxidative reactions starting from a boron compound (e.g. an hydride); however, this could be of minor relevance, because only a small amount of boron is present here. Probably some other element, which was assumed to be in an oxide form is, on the contrary, originally present in the paste in a form which can take up oxygen. Further investigations are required in order to clarify this point. WDS and XRD data suggest that in films fired up to 750° C nickel should be ruled out from the series of species responsible for the weight gains; on the other hand, XRD data suggest that the formation of NiO could be responsible for the weight gain at around 830° C.

Other compounds of nickel, aluminium and boron are formed which allow interconnection of the nickel grains which are not properly sintered, because neither grain growth, nor intergrain necks were observed, in agreement with findings of other authors [11].

The adhesion between alumina substrate and samples seems to derive from interactions of alumina and the "glass-like" matrix; this contention comes from the observation of an increased content of aluminium in the film, as well as the segregation of lead near the film/substrate interface.

The final structure of nickel-based films is, in any case, very complex. Nickel grains are not properly sintered and mixed with various crystalline phases made of nickel, aluminium and boron, in addition to being covered in glass. Nevertheless, their interconnection is sufficient to give a relatively high conductivity and their TCR values are quite similar to that of plain nickel. Even in the case of NiO formation in E2 samples at high temperatures (Figs 2, 4, 5), the sheet resistance does not increase (Fig. 8) probably because lithium dopes NiO. In this case the doped

oxide behaves like a low-resistivity semiconductor [12].

In conclusion, these investigations have proved that nickel-based air-firable thick films with relatively high conductivity can be prepared when the paste contains some species which adequately compete with nickel oxidation.Two types of competitor have been found: boron (three pastes) and elements or compounds which form a lithia–silicate glass at low temperature (one paste).

Acknowledgements

This work was partially supported by Gruppo Nazionale Struttura della Materia, CNR, Italy and Ministero della Pubblica Istruzione, Italy. We thank Dr G. Vezzalini, Institute of Mineralogy, Modena, for WDS analyses, Dr L. Moro, IRST, Povo, Trento, for SIMS experiments, and Dr P. L. Fabbri, CIGS, Modena, for assistance in SEM, EDS experiments.

References

1. R. D. JONES, "Hybrid Circuit Design and Manufacture" (Marcell Dekker, New York, 1982).
2. J. J. COX Jr, *Solid State Technol.* **23** October (1980) 150.
3. S. J. STEIN, C. HUANG and L. CHANG, "Base Metal Thick Film Conductors", Proceedings of the International Society for Hybrid Microelectronics Conference, New York, 1980. (International Society for Hybrid Microelectronics, Montgomery, Alabama, 1980) pp. 58–65.
4. F. FORLANI, in Proceedings of the 4th International Society for Hybrid Microelectronics Conference (Frede Rasmussen, Copenhagen, 1983) pp. 165–177.
5. R. N. LESNICK and M. SPECTOR, in Proceedings of SAE Sensors and Activators Conference, Detroit, pp. 53–57.
6. W. VERMEIRSCH, G. SPEYBROUCK, R. VLAEMINCK, M. HINOUL, R. GOVAERTS and J. VENNIK, in Proceedings of the 4th International Society for Hybrid Microelectronics Conference (Frede Rasmussen, Copenhagen, 1983) pp. 219–30.
7. F. FRANCOVILLE and M. AURAY, in Proceedings of the 4th International Society for Hybrid Microelectronics Conference (Frede Rasmussen, Copenhagen, 1983) pp. 174–87.
8. B. MORTEN, M. PRUDENZIATI, M. SACCHI and F. SIROTTI, *J. Appl. Phys.* **63** (1988) 2267.
9. "Handbook of Chemistry and Physics", 64th Ed (The Chemical Rubber Co., Cleveland, Ohio, 1983/84).
10. C. Y. KUO, in Proceedings of the International Symposium on Microelectronics, Anheim, California (International Society for Hybrid Microelectronics, 1985) pp. 472–77.
11. J. DEGRAEUWE, E. BRAUNS, R. VAN OVERSTRAETEN, J. ROOS and R. GOVAERTS, in Proceedings of the 2nd International Society for Hybrid Microelectronics Conference, Ghent (Dutch Efficiency Bureau, 1979) pp. 295–303.
12. A. J. BOSMAN and C. CREVECOEUR, *Phys. Rev.* **144** (1966) 763.

Received 29 June
and accepted 1 December 1989